International Journal of Heat and Mass Transfer 54 (2011) 1506–1519

Contents lists available at ScienceDirect

International Journal of Heat and Mass Transfer

journal homepage: www.elsevier.com/locate/ijhmt

Inverse analysis with integral transformed temperature fields: Identification of thermophysical properties in heterogeneous media

Carolina P. Naveira-Cotta, Renato M. Cotta *, Helcio R.B. Orlande

Laboratory of Transmission and Technology of Heat-LTTC, Mechanical Eng. Dept. – POLI & COPPE/UFRJ, Universidade Federal do Rio de Janeiro, Rio de Janeiro, RJ, CEP.21945-970, Brazil

ARTICLE INFO

Article history:
Received 28 April 2010
Received in revised form 11 November 2010
Accepted 11 November 2010
Available online 7 January 2011

Keywords:
Integral transforms
Heterogeneous media
Heat conduction
Inverse problem
Thermophysical properties
Bayesian inference

ABSTRACT

The objective of this work is to introduce the use of integral transformed temperature measured data for the solution of inverse heat transfer problems, instead of the common local transient temperature measurements. The proposed approach is capable of significantly compressing the measured data through the integral transformation, without losing the information contained in the measurements and required for the solution of the inverse problem. The data compression is of special interest for modern measurement techniques, such as the infrared thermography, that allows for fine spatial resolutions and large frequencies, possibly resulting on a very large amount of measured data. In order to critically address the use of integral transformed measurements, we examine in this paper the simultaneous estimation of spatially variable thermal conductivity and thermal diffusivity in one-dimensional heat conduction within heterogeneous media. The direct problem solution is analytically obtained via integral transforms and the related eigenvalue problem is solved by the Generalized Integral Transform Technique (GITT). The inverse problem is handled with Bayesian inference by employing a Markov Chain Monte Carlo (MCMC) method. The unknown functions appearing in the formulation are expanded in terms of eigenfunctions as well, so that the unknown parameters become the corresponding series coefficients. Such projection of the functions in an infinite dimensional space onto a parametric space of finite dimension also permits that several quantities appearing in the solution of the direct problem be analytically computed. Simulated measurements are used in the inverse analysis; they are assumed to be additive, uncorrelated, normally distributed, with zero means and known covariances. Both Gaussian and non-informative uniform distributions are used as priors for demonstrating the robustness of the estimation procedure.

1. Introduction

The analysis of diffusion problems in heterogeneous media involves formulations with spatial variations of the thermophysical properties in different ways, such as large scale variations in functionally graded materials (FGM), abrupt variations in layered composites, and random variations due to local concentration fluctuations in dispersed phase systems [1–6]. For instance, composite materials have been providing engineers with increased opportunities for tailoring structures to meet a variety of property and performance requirements. As the composite material morphology in applications presents endless possibilities due to design and manufacturing processes, the characterization of their physical properties is to be made almost case to case [7–13].

The accurate representation of the heat conduction phenomena requires a detailed local solution of the temperature distribution, generally with the aid of discrete numerical solutions with sufficient mesh refinement and computational effort and/or semi-analytical approaches for specific or simplified functional forms. Analytical solutions of linear diffusion problems have been analyzed and compiled in [14], where seven different classes of heat and mass diffusion formulations are systematically solved by the classical Integral Transform Method. The obtained formal solutions are applicable over a very broad range of problems in heat and mass transfer, in part illustrated in the referred compendium. Later on, the classical integral transform approach gained a hybrid numerical–analytical implementation and is in general referred to as the Generalized Integral Transform Technique (GITT) [15–21], offering more flexibility in handling non-transformable problems, including, among others, the analysis of nonlinear diffusion and convection–diffusion problems.

The usefulness of such direct problem solutions is nevertheless limited by the precise knowledge of the corresponding thermophysical properties and boundary condition coefficients that are fed in the corresponding models, and quite often need to be determined by the appropriate inverse problem analysis [22–29]. Among the various available solution techniques of inverse problems [30–34], a fairly common approach is related to the

* Corresponding author.
E-mail addresses: cpncotta@hotmail.com (C.P. Naveira-Cotta), cotta@mecanica.coppe.ufrj.br (R.M. Cotta), helcio@mecanica.coppe.ufrj.br (H.R.B. Orlande).

0017-9310/$ - see front matter © 2010 Elsevier Ltd. All rights reserved.
doi:10.1016/j.ijheatmasstransfer.2010.11.042

Nomenclature

a	coefficient in time lag function of applied heat flux, Eq. (24c)
b	coefficient in time lag function of applied heat flux, Eq. (24c)
c_p	specific heat, Eq. (1.a)
$d(x)$	linear dissipation operator coefficient, Eq. (3.a)
$f(t)$	time lag function in applied heat flux, Eq. (24a)
$h_{eff}(x)$	effective heat transfer coefficient, Eq. (1.a)
$k(x)$	space variable thermal conductivity, Eq. (1.a)
L_x	plate length
L_z	plate thickness
M	truncation order in eigenvalue problem expansion
M_n	normalization integrals in auxiliary eigenvalue problem
N_T	truncation order in temperature expansion
N_w, N_k	truncation orders in coefficients expansions, $w(x)$ and $k(x)$, respectively
N_{Fk}, N_{Fw}, N_{Fd}	number of parameters to be estimated in each filtered solution, $wf(x)$, $kf(x)$ and $df(x)$, respectively
N_{Pk}, N_{Pw}, N_{Pd}	number of parameters to be estimated in each parametrization, $w(x)$, $k(x)$ and $d(x)$, respectively
N_f	number of parameters to be estimated in time behavior of the applied heat flux, $f(t)$
N_P	number of parameters to be estimated, Eq. (20b)
N_x	number of measurements along the spatial domain (sensors)
N_t	number of measurements in time
N_m	total number of measurements
N_i	normalization integrals in original eigenvalue problem
$P(x, t)$	source term, Eq. (3.a,g)
$q_w(x, t)$	applied heat flux, Eq. (1.a)
q_{inf}	heat flux dissipated from electrical resistance, Eq. (24.b)
t	time variable
$T_m(x, t)$	temperature distribution
$w(x)$	thermal capacity, Eq. (3.a)
$w_f(x)$	filter for thermal capacity expansion
x	space coordinate
$\mathbf{Y}$	vector of measurements
$\mathbf{P}$	vector of unknown parameters
$\mathbf{P_w}$, $\mathbf{P_k}$, $\mathbf{P_d}$, $\mathbf{P_f}$	vector of unknown parameters for $w(x)$, $k(x)$, $d(x)$ and $f(t)$ respectively
$\mathbf{T}$	vector of estimated temperatures
$\mathbf{W}$	covariance matrix of the measurement errors

Greek symbols

γ	parameter in heat flux or linear dissipation coefficient spatial variation
ε	emissivity
λ	eigenvalues of the auxiliary problem
μ	eigenvalues of the original problem
ψ	eigenfunctions of the original problem
Ω	eigenfunctions of the auxiliary problem
ρ	density

Subscripts and Superscripts

i, n, m	order of eigenquantities
–	integral transform
$\sim$	normalized eigenfunction
d	dispersed phase (filler) properties
f	filtering function in the coefficient expansion
m	matrix phase properties

minimization of an objective function that usually involves the quadratic difference between measured and estimated dependent variables, such as the least squares norm, or its modified versions with the addition of regularization terms. Although very popular and useful in many situations, the minimization of the least squares norm is a non-Bayesian estimator. A Bayesian estimator is basically concerned with the analysis of the posterior probability density, which is the conditional probability of the parameters given the measurements, while the likelihood is the conditional probability of the measurements given the parameters [33]. If we assume the parameters and the measurement errors to be independent Gaussian random variables, with known means and covariance matrices, and that the measurement errors are additive, a closed form expression can be derived for the posterior probability density. In this case, the estimator that maximizes the posterior probability density can be recast in the form of a minimization problem involving the maximum a posteriori objective function. On the other hand, if different prior probability densities are assumed for the parameters, so that the Posterior Probability Distribution may not allow an analytical treatment, Markov Chain Monte Carlo (MCMC) methods are required to draw samples of all possible parameters, and thus inference on the posterior probability becomes inference on the samples.

In this work we use Bayesian inference for the estimation of spatially variable equation and boundary condition coefficients in diffusion problems, by employing the method of Markov Chain Monte Carlo (MCMC) [33,35–38]. The Metropolis-Hastings algorithm is employed for the sampling procedure [39,40], implemented in the *Mathematica* platform [41]. This sampling procedure used to recover the posterior distribution is in general the most expensive computational task in solving an inverse problem by Bayesian inference, since the direct problem is calculated for each state of the Markov Chain. In this context, the use of a fast, accurate and robust computational implementation of the direct solution [42] is extremely important. Thus, the integral transformation approach discussed above becomes very attractive for the combined use with the Bayesian estimation procedure, since all required expressions in the method are analytically obtained at once by symbolic computation and the single numerical repetitive task is the solution of an algebraic matrix eigenvalue problem [42–44]. Also, instead of seeking the function estimation in the form of a sequence of local values for the variable coefficients, an alternative approach is utilized based on the eigenfunction expansion of the functions to be estimated [42]. As a result, the solution of the inverse problem is performed in a finite dimensional space of parameters, involving the corresponding series coefficients.

The main contribution of the present work is the analysis of the inverse problem in the transformed temperature field, instead of employing the directly measured temperature data. The experimental temperature values at each time are integral transformed along the spatial domain to yield transformed temperature measurements of increasing order, which is the eigenvalue order of the auxiliary problem used in the transformation. This procedure is particularly advantageous when a substantial amount of experimental measurements are available, such as in thermographic sensors, thus permitting a remarkable data compression through the integral transformation process, without discarding any of the available measurements.

In order to demonstrate the applicability of the proposed estimation approach, a simulated experiment is used, which employs

a partially heated thin plate. Natural convection and radiation cooling is considered in the non-heated surface of the plate. It is assumed that infrared camera thermography is utilized to provide a fairly large number of transient temperature measurements over the plate non-heated surface. A combination of uniform and Gaussian priors are employed in the MCMC algorithm, and the thermophysical properties are then estimated for a heterogeneous composite material in the form of an exponential variation of the dispersed phase concentration.

2. Direct problem

We consider a one-dimensional special case of the general formulation on transient heat conduction presented in [42], for the temperature field $T_m(x,t)$ in a region $x \in [0, L_x]$, as depicted in Fig. 1. The formulation includes spatially variable thermal conductivity and heat capacity, $k(x)$ and $w(x)$, respectively. The heat conduction equation with the appropriate initial and boundary conditions are given by:

$$w(x)\frac{\partial T_m(x,t)}{\partial t} = \frac{\partial}{\partial x}\left(k(x)\frac{\partial T_m(x,t)}{\partial x}\right) - \frac{h_{\text{eff}}(x)}{L_z}(T_m(x,t) - T_\infty) + \frac{q_w(x,t)}{L_z}, \quad 0 < x < L_x, \ t > 0 \tag{1a}$$

$$T_m(x,0) = T_\infty \tag{1b}$$

$$\left.\frac{\partial T_m(x,t)}{\partial x}\right|_{x=0} = 0, \quad t > 0 \qquad \left.\frac{\partial T_m(x,t)}{\partial x}\right|_{x=L_x} = 0, \quad t > 0 \tag{1c,d}$$

Problem (1) models a typical one-dimensional transient heat conduction experimental setup for a thermally thin plate, including prescribed heat flux at one surface and convective heat losses at the opposite surface, based on a lumped formulation across the sample thickness. Before providing the integral transform solution of problem (1), a simple filtering solution is employed for improved convergence behavior of the eigenfunction expansions, in the form:

$$T_m(x,t) = T_\infty + T^*(x,t) \tag{2}$$

The filtered temperature formulation is then given by:

$$w(x)\frac{\partial T^*(x,t)}{\partial t} = \frac{\partial}{\partial x}\left(k(x)\frac{\partial T^*(x,t)}{\partial x}\right) - d(x)T^*(x,t) + P(x,t), \quad 0 < x < L_x, \ t > 0 \tag{3a}$$

$$T^*(x,0) = 0$$
$$\left.\frac{\partial T^*(x,t)}{\partial x}\right|_{x=0} = 0, \qquad \left.\frac{\partial T^*(x,t)}{\partial x}\right|_{x=L} = 0, \quad t > 0 \tag{3b-d}$$

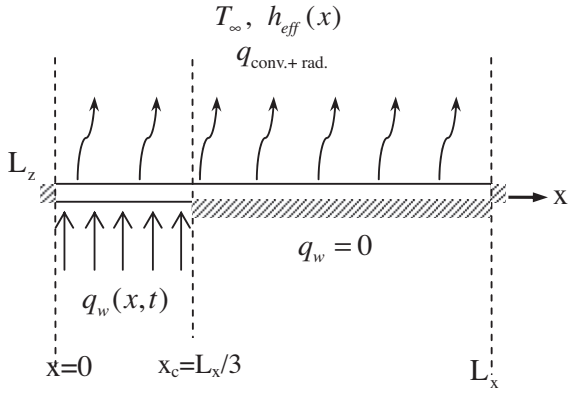

Fig. 1. Physical problem.

where

$$w(x) = \rho(x)c_p(x); \quad d(x) = \frac{h_{\text{eff}}(x)}{L_z}; \quad P(x,t) = \frac{q_w(x,t)}{L_z} \tag{3e-g}$$

The formal exact solution of problem (1) is then obtained with the Classical Integral Transform Method [14], and is written as:

$$T_m(x,t) = T_\infty + \sum_{i=1}^{\infty}\tilde{\psi}_i(x)\int_0^t \bar{g}_i(t')e^{-\mu_i^2(t-t')}dt \tag{4}$$

where the eigenvalues μ_i and eigenfunctions $\psi_i(x)$, are obtained from the eigenvalue problem that contains the information about the heterogeneous medium, in the form:

$$\frac{d}{dx}\left[k(x)\frac{d\psi_i(x)}{dx}\right] + (\mu_i^2 w(x) - d(x))\psi_i(x) = 0, \quad x \in [0, L_x] \tag{5a}$$

with boundary conditions

$$\frac{d\psi_i(x)}{dx} = 0, \quad x = 0, \qquad \frac{d\psi_i(x)}{dx} = 0, \quad x = L_x \tag{5b,c}$$

Also, the other quantities that appear in the exact solution (4) are computed after solving problem (5), such as:

$$\tilde{\psi}_i(x) = \frac{\psi_i(x)}{\sqrt{N_i}}, \quad \text{normalized eigenfunctions} \tag{6a}$$

$$N_i = \int_0^{L_x} w(x)\psi_i^2(x)dx, \quad \text{normalization integrals} \tag{6b}$$

$$\bar{g}_i(t) = \int_0^{L_x} P(x,t)\tilde{\psi}_i(x)dx, \quad \text{transformed source terms} \tag{6c}$$

The Generalized Integral Transform Technique (GITT) is here employed for the solution of the Sturm–Liouville problem (5) via the proposition of a simpler auxiliary eigenvalue problem, and expanding the unknown eigenfunctions in terms of the chosen basis [42–44]. Also, the variable equation coefficients are themselves expanded in terms of known eigenfunctions [42], so as to allow for a fully analytical implementation of the coefficients matrices in the transformed system. The solution of problem (5) is thus proposed as an eigenfunction expansion, in terms of the following simpler auxiliary eigenvalue problem:

$$\frac{d^2\Omega_n(x)}{dx^2} + \lambda_n^2\Omega_n(x) = 0, \quad x \in [0, L_x] \tag{7a}$$

with boundary conditions

$$\frac{d\Omega_n(x)}{dx} = 0, \quad x = 0, \qquad \frac{d\Omega_n(x)}{dx} = 0, \quad x = L_x \tag{7b,c}$$

with normalized eigenfunctions, eigenvalues and norms given by:

$$\tilde{\Omega}_n(x) = \frac{\cos(\lambda_n x)}{\sqrt{M_n}}, \quad \lambda_n = \frac{n\pi}{L_x}, \quad \text{with } n = 0, 1, 2, \ldots$$
$$M_0 = L_x \quad \text{and} \quad M_n = \frac{L_x}{2}, \quad \text{with } n = 1, 2, \ldots \tag{8a-d}$$

The proposed expansion of the original eigenfunction is then given by:

$$\psi_i(x) = \sum_{n=1}^{\infty}\tilde{\Omega}_n(x)\bar{\psi}_{i,n}, \quad \text{inverse} \tag{9a}$$

$$\bar{\psi}_{i,n} = \int_0^{L_x}\psi_i(x)\tilde{\Omega}_n(x)dx, \quad \text{transform} \tag{9b}$$

The integral transformation is thus performed by operating Eq. (3a) on with $\int_0^{L_x}\tilde{\Omega}_n(x) - dx$, to yield, after some manipulation [42–44], the following algebraic problem in matrix form:

$$(\mathbf{A} - v\mathbf{B})\bar{\psi} = 0, \quad \text{with } v = \mu^2 \tag{10a}$$

$$\bar{\psi} = \bar{\psi}_{n,m}; \quad \mathbf{B} = \{B_{n,m}\}, \quad B_{n,m} = \int_0^{L_x} w(x)\tilde{\Omega}_n(x)\tilde{\Omega}_m(x)dx \tag{10b-d}$$

$$\mathbf{A} = \{A_{n,m}\},$$

$$A_{n,m} = \int_0^{L_x} \tilde{\Omega}_m(x)\frac{d}{dx}\left[k(x)\frac{d\tilde{\Omega}_n(x)}{dx}\right]dx - \int_0^{L_x} d(x)\tilde{\Omega}_n(x)\tilde{\Omega}_m(x)dx \tag{10e, f}$$

The algebraic problem (10a) can be numerically solved to provide results for the eigenvalues and eigenvectors, upon truncation to a sufficiently large finite order M, which will be combined by the inverse formula (9a) to provide the desired original eigenfunctions. It is also of interest to express the variable coefficients themselves as eigenfunction expansions [42]. This is particularly advantageous in the evaluation of the algebraic system coefficients, $A_{n,m}$ and $B_{n,m}$. All the related integrals can then be expressed in terms of eigenfunctions, allowing for straightforward analytical evaluations. For instance, the coefficient $w(x)$ can be expanded in terms of eigenfunctions, together with a filtering solution to enhance convergence, in the following form:

$$w(x) = w_f(x) + \sum_{k=1}^{\infty} \tilde{\Gamma}_k(x)\bar{w}_k, \quad \text{inverse} \tag{11a}$$

$$\bar{w}_k = \int_0^{L_x} \hat{w}(x)[w(x) - w_f(x)]\tilde{\Gamma}_k(x)dx, \quad \text{transform} \tag{11b}$$

where $\hat{w}(x)$ is the weighting function for the chosen normalized eigenfunction $\tilde{\Gamma}_k(x)$. This eigenfunction basis may be chosen from the same auxiliary problem equation, but with first order boundary conditions, while the filtering function may be a simple analytic function that satisfies the boundary values for the original coefficients. The two remaining coefficients are equally expanded, in terms of eigenfunctions, to yield:

$$k(x) = k_f(x) + \sum_{k=1}^{\infty} \tilde{\Gamma}_k(x)\bar{k}_k, \quad \text{inverse} \tag{11c}$$

$$\bar{k}_k = \int_0^{L_x} \hat{w}(x)[k(x) - k_f(x)]\tilde{\Gamma}_k(x)dx, \quad \text{transform} \tag{11d}$$

$$d(x) = d_f(x) + \sum_{k=1}^{\infty} \tilde{\Gamma}_k(x)\bar{d}_k, \quad \text{inverse} \tag{11e}$$

$$\bar{d}_k = \int_0^{L_x} \hat{w}(x)[d(x) - d_f(x)]\tilde{\Gamma}_k(x)dx, \text{transform} \tag{11f}$$

The matrices coefficients may then be rewritten in terms of the expanded functions, such as for the elements of matrix B:

$$B_{n,m} = \int_0^{L_x} w_f(x)\tilde{\Omega}_n(x)\tilde{\Omega}_m(x)dx + \sum_{k=1}^{\infty} \bar{w}_k \int_0^{L_x} \tilde{\Gamma}_k(x)\tilde{\Omega}_n(x)\tilde{\Omega}_m(x)dx \tag{12a}$$

and for matrix A:

$$A_{n,m} = \int_0^{L_x} \tilde{\Omega}_m(x)\frac{d}{dx}\left[k_f(x)\frac{d\tilde{\Omega}_n(x)}{dx}\right]dx + \sum_{k=1}^{\infty}\left[\int_0^{L_x} \tilde{\Omega}_m(x)\frac{d}{dx}\left[\tilde{\Gamma}_k(x)\frac{d\tilde{\Omega}_n(x)}{dx}\right]dx\right]\bar{k}_k - \int_0^{L_x} d_f(x)\tilde{\Omega}_n(x)\tilde{\Omega}_m(x)dx - \sum_{k=1}^{\infty}\left[\int_0^{L_x} \tilde{\Gamma}_k(x)\tilde{\Omega}_n(x)\tilde{\Omega}_m(x)dx\right]\bar{d}_k \tag{12b}$$

Also, the normalization integrals are then computed from:

$$N_i = \sum_{n=1}^{\infty}\sum_{m=1}^{\infty}\bar{\psi}_{i,n}\bar{\psi}_{i,m}\left\{\int_0^{L_x} w_f(x)\tilde{\Omega}_n(x)\tilde{\Omega}_m(x)dx + \sum_{k=1}^{\infty}\left[\int_0^{L_x} \tilde{\Gamma}_k(x)\tilde{\Omega}_n(x)\tilde{\Omega}_m(x)dx\right]\bar{w}_k\right\} \tag{12c}$$

3. Inverse problem

For the solution of the inverse problem, we assume available a vector of measurements $\mathbf{Y}$, whose values are uncertain and described by a probability distribution with density $p(\mathbf{Y}|\mathbf{P})$. The quantity $\mathbf{P}$ indexes the family of observation distributions representing characteristics of interest. However, the quantity $\mathbf{P}$ may be more than a simple indexer and may be the very reason of taking measurements, if the goal of the analysis is the determination of its value. In addition, it is possible that prior knowledge about the quantity $\mathbf{P}$ be available, so that it can be incorporated into the analysis through a distribution $p(\mathbf{P})$ within the Bayesian framework [35].

In this way, the process of inference is based on the distribution of probability $\mathbf{P}$ after observing the value of $\mathbf{Y}$, which becomes part of the available information as a whole. The distribution $p(\mathbf{P}|\mathbf{Y})$ is called the *a posteriori* distribution, in direct opposition to the *a priori* distribution, and can be obtained through Bayeś theorem as:

$$p(\mathbf{P}|\mathbf{Y}) = \frac{p(\mathbf{Y}|\mathbf{P})p(\mathbf{P})}{p(\mathbf{Y})} \propto p(\mathbf{Y}|\mathbf{P})p(\mathbf{P}) \tag{13}$$

where the probability distribution $p(\mathbf{Y})$ plays the role of a normalizing constant [33,35,36].

Once we have obtained the *a posteriori* distribution within the proportionality constant, the information contained therein can be summarized by statistical measures, in particular to provide estimates of central values and dispersion. The main positioning quantities are the average, median and mode, and the key quantities for the dispersion are the variance, the standard deviation, and the precision and curvature of the mode. The relationship among these quantities and their relationship with the rules of decision are given by Migon and Gamerman [36].

By assuming that the temperature data are additive, uncorrelated, Gaussian, with zero mean and constant standard deviation $\sigma_{\mathbf{Y}}$, the likelihood can be written as:

$$p(\mathbf{Y}|\mathbf{P}) = \frac{1}{(2\pi\sigma_{\mathbf{Y}}^2)^{-1/2}}\exp\left[-\frac{(\mathbf{Y} - \mathbf{T}(\mathbf{P}))^T(\mathbf{Y} - \mathbf{T}(\mathbf{P}))}{2\sigma_{\mathbf{Y}}^2}\right] \tag{14}$$

where $\mathbf{T}$ is the vector of calculated temperatures as a function of the parameters to be estimated, and $\mathbf{Y}$ are the measured temperatures.

The unknown quantities in the diffusion problem addressed here are the variable equation coefficients and eventually also the space variable effective heat transfer coefficient. Remember, however, that the approach adopted in solving the direct problem was to expand such coefficients in terms of eigenfunctions, so that the unknown quantities are in fact the coefficients of the eigenfunction expansion and the two values of the properties at the boundaries, employed in the solution procedure as a filter.

When it is not possible to analytically obtain the corresponding marginal distributions, one needs to use a method based on

simulation [35]. Inference based on simulation techniques uses samples from the posteriori $p(\mathbf{P}|\mathbf{Y})$ to extract information about $\mathbf{P}$. The numerical method most used to explore the space of states of the posteriori is the Monte Carlo simulation. The Monte Carlo simulation is based on a large sample of the probability density function (in this case, the function of the posterior probability density $p(\mathbf{P}|\mathbf{Y})$). Several sampling strategies are proposed in the literature, including the Monte Carlo method by Markov Chain (MCMC) adopted in this work, where the basic idea is to simulate a random walk in the space of $p(\mathbf{P}|\mathbf{Y})$ that converges to a stationary distribution, which is the distribution of interest in the problem.

A Markov chain is a stochastic process $\{\mathbf{P}_0, \mathbf{P}_1, \ldots\}$ such that the distribution of $\mathbf{P}_i$, given all previous values $\mathbf{P}_0, \ldots, \mathbf{P}_{i-1}$, depends only on $\mathbf{P}_{i-1}$. A Markov chain is more precisely defined by its transition probability $p(i,j) = p(i \to j)$, which defines the probability that the process, from the state s_i moves to the state s_j in a single step, as follows:

$$p(i,j) = p(i \to j) = p(\mathbf{P}_{t+1} = s_j | \mathbf{P}_t = s_i) \tag{15}$$

The MCMC methods require, in order to obtain a single equilibrium distribution, that the Markov chain be [35]:

- homogeneous, that is, the probability of transition from one state to another is invariant;
- irreducible, that is, each state can be reached from any other in a finite number of iterations;
- aperiodic, that is, there are no absorbing states.

A sufficient condition for a single equilibrium distribution is that the process meets the following balance equation:

$$p(i \to j) p_i(\mathbf{P}|\mathbf{Y}) = p(j \to i) p_j(\mathbf{P}|\mathbf{Y}) \tag{16}$$

where $p(\mathbf{P}_i|\mathbf{Y})$ and $p(\mathbf{P}_j|\mathbf{Y})$ are the posterior probabilities of different states of the distribution of interest.

The most commonly used MCMC algorithms are the Metropolis-Hastings, here employed, and the Gibbs sampler [35,36]. The Markov chain Monte Carlo method according to the generic label of Metropolis-Hastings, comes from the articles of Metropolis et al. [39] and Hastings [40], later on complemented by several relevant works. The Metropolis-Hastings algorithm uses the same idea of the rejection methods, i.e., a value is generated from an auxiliary distribution and accepted with a given probability. This correction mechanism ensures the convergence of the chain for the equilibrium distribution. The Metropolis-Hastings algorithm uses an auxiliary probability density function, $q(\mathbf{P}*|\mathbf{P})$, from which it is easy to obtain sample values. Assuming that the chain is in a state $\mathbf{P}$, a new candidate value, $\mathbf{P}*$, is generated from the auxiliary distribution $q(\mathbf{P}*|\mathbf{P})$, given the current state of the chain $\mathbf{P}$, where $\mathbf{P}$ is the vector of parameters under study.

The new value $\mathbf{P}*$ is accepted with probability given by Eq. (17), where the ratio that appears in this equation was called by Hastings [40] the ratio test, being today called the ratio of Hastings "RH"

$$RH(\mathbf{P}, \mathbf{P}^*) = \min\left[1, \frac{p(\mathbf{P}^*|\mathbf{Y}) q(\mathbf{P}^*|\mathbf{P})}{p(\mathbf{P}|\mathbf{Y}) q(\mathbf{P}|\mathbf{P}^*)}\right] \tag{17}$$

where $p(\mathbf{P}|\mathbf{Y})$ is the *a posteriori* distribution of interest. An important observation is that we only need to know $p(\mathbf{P}|\mathbf{Y})$ up to a constant, since we are working with ratios between densities and the normalization constant, Eq. (13), is cancelled.

In practical terms, the simulation of a sample of $p(\mathbf{P}|\mathbf{Y})$ using the Metropolis-Hastings algorithm can be outlined as follows [35]:

1. Boot up the iterations counter of the chain $i = 0$ and assign an initial value $\mathbf{P}^{(0)}$.
2. Generate a candidate value $\mathbf{P}^*$of the distribution $q(\mathbf{P}^*/\mathbf{P})$.
3. Calculate the probability of acceptance of the candidate value $RH(\mathbf{P}, \mathbf{P}^*)$ by Eq. (17).
4. Generate a random number u with uniform distribution, i.e., $u \sim U(0,1)$.
5. If $u \leqslant$ RH then the new value is accepted and we let $\mathbf{P}^{(i+1)} = \mathbf{P}^*$, otherwise the new value is rejected and we let $\mathbf{P}^{(i+1)} = \mathbf{P}^{(i)}$.
6. Increase the counter i to $i + 1$ and return to step 2.

The transition core $q(\mathbf{P}^*|\mathbf{P})$ defines the proposal for a movement that can be confirmed or not by $RH(\mathbf{P}, \mathbf{P}^*)$. For this reason $q(\mathbf{P}^*|\mathbf{P})$ is usually called the proposal and, when regarded as a conditional density, it is called the proposal density (or distribution) [35].

In this study we have chosen to adopt symmetrical chains, i.e., $q(\mathbf{P}^*|\mathbf{P}) = q(\mathbf{P}|\mathbf{P}^*)$ for all $(\mathbf{P}^*, \mathbf{P})$. In this case, Eq. (17) reduces to the ratio of the posterior densities calculated at the previous and proposed chain positions, and does not depend on $q(\mathbf{P}^*|\mathbf{P})$.

4. Integral transformation of the measured data

The main objective of the present study was to advance the solution of the inverse problem in the transformed temperature field, from the integral transformation of the experimental temperature data. With such an approach, the experimental measurements in the spatial domain are compressed into few transformed modes, as it will be apparent below. Once the experimental temperature readings $\mathbf{Y}$ have been obtained, one proceeds to the integral transformation of the temperature field at each measured time. For this purpose the temperature measurements can be interpolated in the

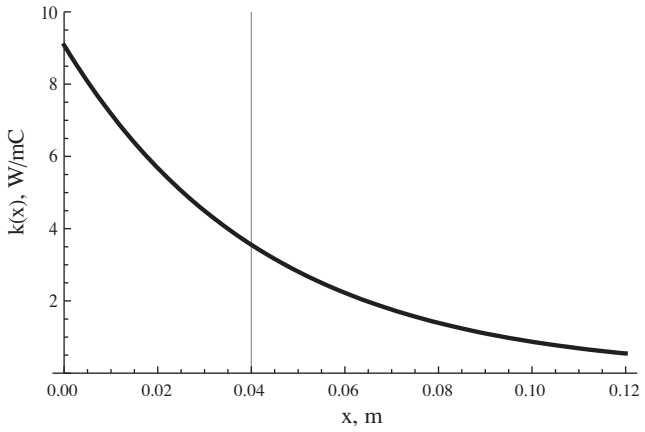

(a) **Thermal conductivity**

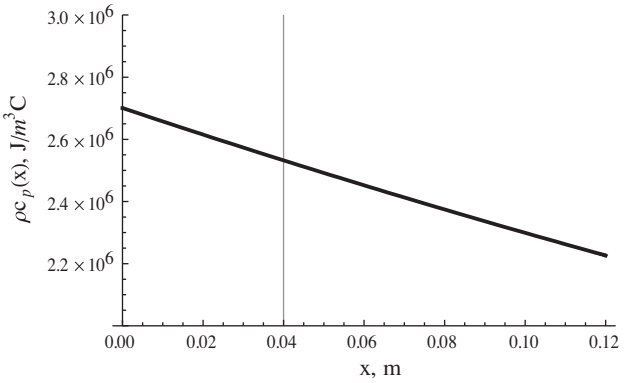

(b) **Volumetric heat capacity**

Fig. 2. Spatial behavior of thermophysical properties: (a) thermal conductivity and (b) volumetric heat capacity.

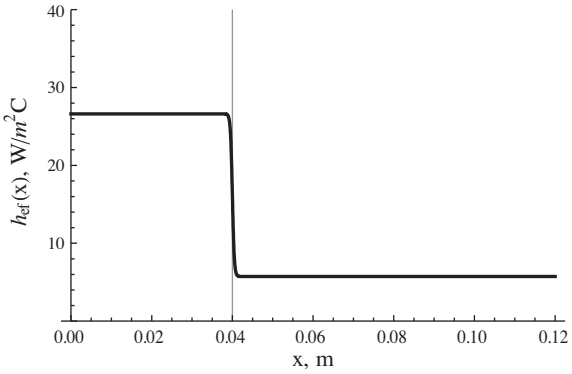

(a) Effective heat transfer coefficient - $h_{eff}(x)$

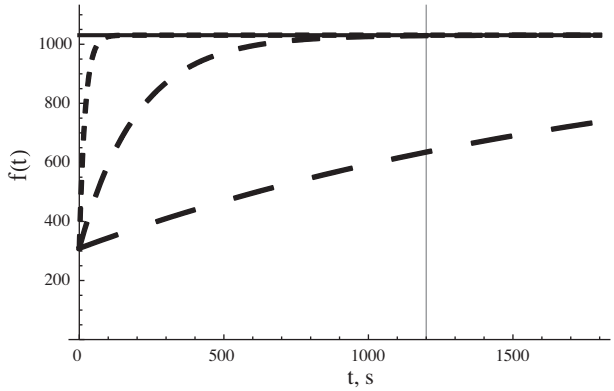

(b) Time lag function in applied heat flux - $f(t)$ for b=0.005, and a=1, lower curve (long dashes); a=0.7, middle curve; a=0.3, upper curve (short dashes); a=0, horizontal curve (solid line)

Fig. 3. Spatial behavior of additional coefficients.

spatial domain, generating the continuous functions $T_{\exp}(x, t)$, which are then integral transformed, according to the following integral transform pair:

$$\text{Transform} \quad \overline{T}_{\exp,i}(t) = \int_0^{L_x} w(x)\tilde{\psi}_i(x)[T_{\exp}(x,t) - T_\infty]dx \tag{18a}$$

$$\text{Inverse} \quad T_{\exp}(x,t) = T_\infty + \sum_{i=0}^{NT} \tilde{\psi}_i(x)\overline{T}_{\exp,i}(t) \tag{18b}$$

In the context of the Bayesian inference here adopted, we thus have to reformulate the likelihood function because the experimental data are now the transformed temperatures, according to Eq. (18a). We compare in Eq. (19) the expressions for the likelihood as traditionally obtained directly from the temperature measurements, Eq. (19a), and as here calculated from the transformed temperature fields, both weighted by the adequate experimental standard deviation in each field.

Likelihood in the temperature field

$$\propto Exp\left[-\frac{1}{2}\sum_{s}^{Nx}\sum_{m}^{Nt}\frac{1}{\sigma_s^2}(T_{\exp}(x_s,t_m) - T_{\text{calc}}(x_s,t_m))^2\right] \tag{19a}$$

Likelihood in the transformed temperature field

$$\propto Exp\left[-\frac{1}{2}\sum_{i}^{NT}\sum_{m}^{Nt}\frac{1}{\overline{\sigma}_i^2}(\overline{T}_{\exp,i}(t_m) - \overline{T}_{\text{calc},i}(t_m))^2\right] \tag{19b}$$

where NT is the number of modes used in representing the transformed temperature.

Table 1
Data employed to generate the simulated experimental data.

t_{final}	3 600 s	ε	0.97
L_x	0.12 m	a	0.7
L_y	0.04 m	b	0.005 s^{-1}
L_z	0.001 m	q_{inf}	1030.9 W/m^2
x_C	0.04 m	T_∞	23.4 °C

Table 2a
Functions and parameters to be estimated for each coefficient.

Coefficient	Adopted function	Numerical parameters
$k(x)$	Eigenfunction expansion	$\mathbf{P}_k^{\mathrm{T}} \equiv [k_{x0}, k_{xL}, \bar{k}_1, \bar{k}_2, \ldots, \bar{k}_{N_k}]$
$w(x)$	Eigenfunction expansion	$\mathbf{P}_w^{\mathrm{T}} \equiv [w_{x0}, w_{xL}, \bar{w}_1, \bar{w}_2, \ldots, \bar{w}_{N_w}]$
$d(x)$	Eigenfunction expansion	$\mathbf{P}_d^{\mathrm{T}} \equiv [d_{x0}, d_{xL}, \bar{d}_1, \bar{d}_2, \ldots, \bar{d}_{N_d}]$
$f(t)$	Parametrization given by Eq. (20.c)	$\mathbf{P}_f^{\mathrm{T}} \equiv [a, b]$

Table 2b
Filters employed for each coefficient representation.

Coefficient	Filter	Functional form	Numerical parameters in filter
$k(x)$	Linear	$\frac{(k_{xL}-k_{x0})}{L_x}x + k_{x0}$	$N_{kF} = 2$
$w(x)$	Linear	$\frac{(w_{xL}-w_{x0})}{L_x}x + w_{x0}$	$N_{wF} = 2$
$d(x)$	Step	$d_{x0} + \frac{d_{xL}-d_{x0}}{1+\exp\left[-\frac{\gamma(x-x_C)}{L_x}\right]}$ For $\gamma = 200$	$N_{dF} = 2$

In a previous contribution [45], the combination of integral transforms and Bayesian inference was presented, aiming at the estimation of spatially variable thermal conductivities in two-phase dispersed systems. Simulated temperature measurements were directly employed in the inverse problem analysis, and prior information in terms of estimates on the dispersed phase concentration was invoked. An example of abrupt space variation was then selected and the approach was extensively tested and demonstrated. Nevertheless, it was then recognized that computational cost could be markedly affected by further increasing the number of sensors and measurements, such as in modern non-intrusive infrared thermography temperature acquisition [38]. Therefore, the present work introduces the inverse problem analysis based on integral transformed experimental data, instead of directly employing the original temperature data, thus compressing the experimental information and significantly reducing computational costs. Also, to further challenge the inverse analysis algorithm, an application has been selected involving exponential variations of thermophysical properties in heterogeneous media, such as in FGM (functionally graded materials), without the need of a priori information on the concentration of the dispersed phase, as described below.

Table 3a
Number of spatial and time measurements used in the sensitivity analysis.

Number of time measurements $N_t = 300$	
Number of spatial measurements, N_x	Total number of experimental points, N_m
61	18 300
121	36 300
241	72 300
481	144 300
961	288 300
1921	576 300

Table 3b
Number of parameters considered in the sensitivity analysis.

Coefficient	Number of parameters		
$k(x)$	$N_{Pk} = 2 + 1$	$N_{Pk} = 2 + 3$	$N_{Pk} = 2 + 5$
$w(x)$	$N_{Pw} = 2 + 1$	$N_{Pw} = 2 + 3$	$N_{Pw} = 2 + 5$
$d(x)$	$N_{Pd} = 2 + 1$	$N_{Pd} = 2 + 1$	$N_{Pd} = 2 + 1$
$f(t)$	$N_f = 2$	$N_f = 2$	$N_f = 2$
Total number of parameters			
N_P	11	15	19

Table 4
Comparison of the number of experimental points for the estimation in the temperature field and in the transformed temperature field.

Number of spatial measurements, N_x	Number of time measurements, N_t	Total number of experimental points, N_m
241	120	25 680
	200	48 200
	300	72 300
Number of modes in temperature expansion	Number of time measurements, N_t	Total number of experimental points, N_m
$NT = 10$	120	1200
	200	2000
	300	3000
$NT = 20$	120	2400
	200	4000
	300	8000
$NT = 40$	120	4800
	200	8000
	300	12 000

5. Results and discussion

The selected physical problem deals with a thermally thin plate of thickness $L_z = 1$ mm heated by an electrical resistance on one surface up to a fraction $x_C = L_x/3$ of its total length, $L_x = 12$ cm. At

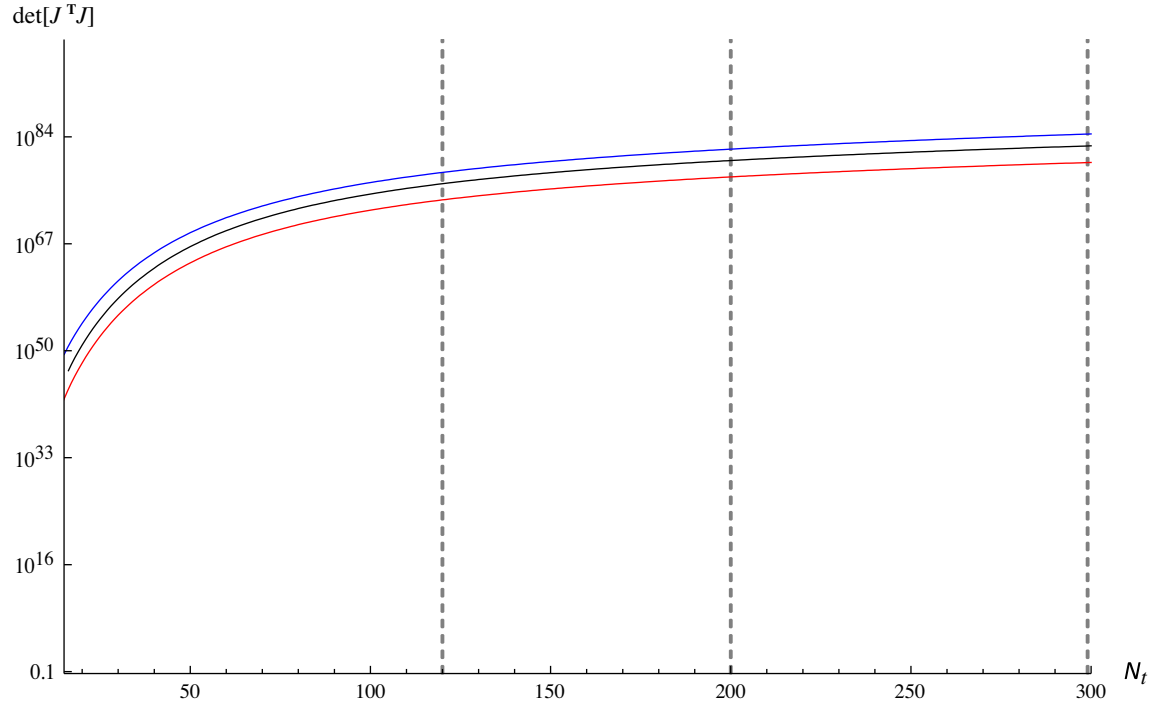

Fig. 4. Determinant of the information matrix for estimation in the transformed temperature field (from top to bottom, $NT = 40$, 20, and 10 terms).

the opposite surface the plate experiences heat losses by both natural convection and radiation, here taken into account in linearized form, while all lateral borders are considered to be insulated. This problem was thus modeled with a one-dimensional transient heat conduction formulation, as described in Eq. (1) and represented in Fig. 1, after lumping in the transversal direction. The power dissipated in the resistance per unit area is considered to be known, $q_{\inf}$, and the spatial distribution of the applied heat flux is also available, being uniform up to $x = x_c$ and zero for $x > x_c$, while an exponential function in time, $f(t)$, models the delay due to the thermal capacitance of the electrical resistance, i.e.:

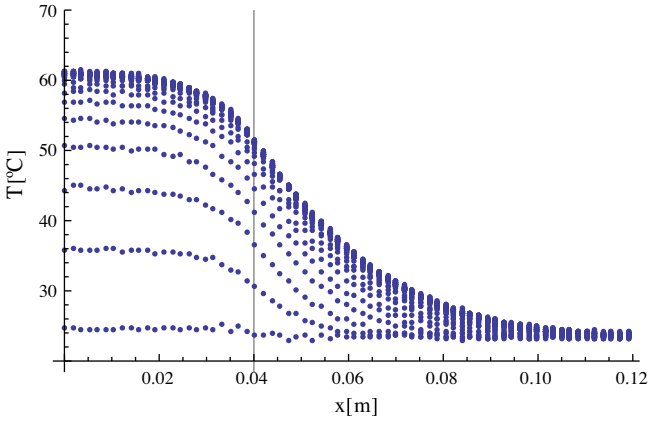

Fig. 5a. Simulated temperature data for selected times, along the plate, for the 0.5 °C uncertainty.

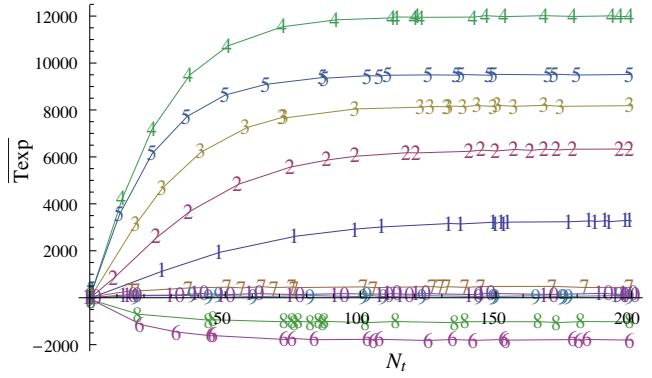

Fig. 5b. Simulated transient variation of the transformed temperature data up to $NT = 10$ and for the 0.5 °C uncertainty (numeric symbols indicate the transformed temperature mode).

$$q_w[x,t] = q[x]f[t] \tag{20a}$$

$$q[x] = \begin{cases} q_{\inf} & 0 < x < L_x/3, \\ 0 & L_x/3 < x < L_x, \end{cases} \quad f[t] = 1 - ae^{-bt} \tag{20b, c}$$

We then seek the simultaneous estimation of the thermal capacity, thermal conductivity, effective heat transfer coefficient, and parameters of the time delay of the applied heat flux, respectively, $w(x)$, $k(x)$, $h_{\text{eff}}(x)$, a and b.

In the present inverse problem analysis, a test-case was chosen in the form of a polymeric matrix (HDPE) with dispersed alumina nanoparticles (Al_2O_3). The concentration of nanoparticles was assumed as an exponential function, varying from essentially the pure polymer at $x = 0$, up to 60% of nanoparticles at $x = L_x$. The polymer volumetric heat capacity and thermal conductivity are respectively of $w_m = 2.2264 \times 10^6$ J/m^3 C and $k_m = 0.545$ W/m C, while the alumina nanoparticles have thermophysical properties given by $w_p = 3.0172 \times 10^6$ J/m^3 C and $k_p = 36$ W/m C. By employing the mixture theory and the Lewis and Nielsen correlation [5,10] to compute the effective volumetric heat capacity and thermal conductivity throughout the domain, we obtain at $x = L_x$, $w_{x=L_x} = 2.7008 \times 10^6$ J/m^3 C and $k_{x=L_x} = 9.078$ W/m C. Therefore, in the present test-case the thermophysical properties were chosen to vary in exponential form as:

$$k(x) = k_0 \exp\left[2\beta_k\left(1 - \frac{x}{L_x}\right)\right], \quad \beta_k = 1.4064$$
$$w(x) = w_0 \exp\left[2\beta_w\left(1 - \frac{x}{L_x}\right)\right], \quad \beta_w = 0.0966 \tag{21a, b}$$

which are illustrated in Fig. 2a and b for the thermal conductivity and volumetric heat capacity, respectively.

The effective heat transfer coefficient was also estimated accounting for natural convection and linearized radiation at the horizontal plate, yielding the behavior shown in Fig. 3a. Fig. 3b illustrates possible behaviors for the time lag in the applied heat flux, by varying the parameter a and fixing $b = 0.005$. The remaining data that define the test-case is then provided in Table 1, from which the simulated experimental data was generated with the direct problem solution.

The convergence of the temperature eigenfunction expansions was analysed for increasing truncation orders, up to $NT = 40$, and full convergence to four significant digits was achieved at these truncation orders. Even for much lower truncation orders ($NT < 15$) it was achieved a three significant digits convergence, which is a quite favorable aspect for the sake of accelerating the solution of the proposed inverse problem.

Table 2a summarizes the parametrization adopted in each function to be estimated and the number of parameters in each case. Table 2b shows the filtering choices for the expanded coefficients, that complement the information on the total number of

Table 5
Test cases examined.

Simulated experimental data ($NT = 10$, $NP_k = 3$, $NP_w = 3$, $NP_d = 3$, $N_f = 2$)					
Case	Temperature uncertainty	NT	N_t	N_x	Prior $k_{x0}, k_{xL}, \bar{k}_j - w_{x0}, w_{xL}, \bar{w}_j - d_{x0}, d_{xL}, \bar{d}_j - a, b$
Validation cases					
1	0.001 °C	10	200	241	N, N, U – N, N, U – N, N, U – U, U
2	0.5 °C	10	200	241	N, N, U – N, N, U – N, N, U – U, U
Simulated experimental data ($NT = 50$, $NP_k = 12$, $NP_w = 12$, $NP_d = 12$, $N_f = 2$)					
Case	Temperature uncertainty	NT	N_t	N_x	Prior $k_{x0}, k_{xL}, \bar{k}_j - w_{x0}, w_{xL}, \bar{w}_j - d_{x0}, d_{xL}, \bar{d}_j - a, b$
Test cases					
3	0.1 °C	10	200	241	N, N, U – N, N, U – N, N, U – U, U
4	0.5 °C	10	200	241	N, N, U – N, N, U – N, N, U – U, U

(*) N – Normal (Gaussian) prior; U – Uniform prior.

Table 6
Input data for estimation.

P	Exact	Min	Max	Initial
k_{x0}	9.0780	0.463	10.440	8.6157
k_{xL}	0.545	0.463	10.440	0.5028
$\bar{k}_1$	−0.6677	−3.111	3.111	−0.7256
$\bar{k}_2$	−0.1111	−0.778	0.778	−0.1082
$\bar{k}_3$	−0.04091	−1.037	1.037	−0.04433
w_{x0}	2.701×10^6	1.892×10^6	3.106×10^6	2.686×10^6
w_{xL}	2.226×10^6	1.892×10^6	3.106×10^6	2.282×10^6
$\bar{w}_1$	−2894.68	−378487.0	378487.0	−2810.39
$\bar{w}_2$	−34.942	−94621.8	94621.8	−33.045
$\bar{w}_3$	−107.57	−126162.0	126162.0	−104.67
h_{x0}	26.620	13.310	53.241	26.601
h_{xL}	5.7286	2.8643	11.457	6.2323
$\bar{h}_1$	0	-3×10^{-12}	3×10^{-12}	0.
$a* = aq_{\inf}$	721.65	0	1 237.1	700.89
b	0.005	0	0.1	0.00521

parameters to be estimated for the functions $k(x)$, $w(x)$, the linear dissipation term $d(x) = h_{\text{eff}}(x)/L_z$ and the time behavior of the applied heat flux, $f(t)$. Therefore, the total number of parameters "NP" is given by the sum of the parameters in each expansion and the respective filters, as follows:

$$\begin{aligned} &\mathbf{P}^{\mathrm{T}} \equiv \mathbf{P}_{\mathrm{k}}^{\mathrm{T}} \cup \mathbf{P}_{\mathrm{w}}^{\mathrm{T}} \cup \mathbf{P}_{\mathrm{d}}^{\mathrm{T}} \cup \mathbf{P}_{\mathrm{f}}^{\mathrm{T}} \\ &N_P = N_{Pk} + N_{Pw} + N_{Pd} + N_f \\ &N_P = (N_{kF} + N_k) + (N_{wF} + N_w) + (N_{dF} + N_d) + N_f \end{aligned} \tag{22a-c}$$

The filters were chosen as functions that incorporate the values of the coefficients at the two boundaries, $x = 0$ and L_x, (k_{x0}, k_{xL}, w_{x0}, w_{xL} and d_{x0}, d_{xL}), which are unknown and should be estimated together with the eigenfunction expansions coefficients, so as to make the boundary conditions of the chosen eigenfunction homogeneous. For the thermophysical properties $k(x)$ and $w(x)$ we have employed a simple linear filter without any sort of *a priori* information on the coefficients variations. For the dissipation coefficient, $d(x)$, a more informative filter was adopted in the form of a steep variation approaching a step function, since this behavior is physically expected, in light of the functional form of the applied heat flux.

Before addressing the estimation of the unknown parameters, the behavior of the determinant of the information matrix $\mathbf{J}^{\mathrm{T}}\mathbf{J}$ [32] needs to be analyzed in order to inspect the influence of the number of parameters to be estimated in the solution of the inverse problem. The sensitivity matrix $\mathbf{J}$ is defined as:

$$\mathbf{J}(\mathbf{P}) = \left[\frac{\partial \mathbf{T}^{\mathrm{T}}(\mathbf{P})}{\partial \mathbf{P}}\right]^{\mathrm{T}} = \begin{bmatrix} \frac{\partial T_1}{\partial P_1} & \frac{\partial T_1}{\partial P_2} & \frac{\partial T_1}{\partial P_3} & \cdots & \frac{\partial T_1}{\partial P_{N_p}} \\ \frac{\partial T_2}{\partial P_1} & \frac{\partial T_2}{\partial P_2} & \frac{\partial T_2}{\partial P_3} & \cdots & \frac{\partial T_2}{\partial P_{N_p}} \\ \vdots & \vdots & \vdots & & \vdots \\ \frac{\partial T_I}{\partial P_1} & \frac{\partial T_I}{\partial P_2} & \frac{\partial T_I}{\partial P_3} & \cdots & \frac{\partial T_I}{\partial P_{N_p}} \end{bmatrix} \tag{23}$$

where, for simplicity, the estimated variables were taken as the actual temperatures and not the ones obtained after the integral transformation as discussed above. The sensitivity coefficients $J_{ij} = \frac{\partial T_i}{\partial P_j}$ give the sensitivity of T_i with respect to changes in the parameter P_j. A small value of the magnitude of J_{ij} indicates that large changes in P_j yield small changes in T_i. It can be easily noticed that the estimation of the parameter P_j is extremely difficult in such cases, because basically the same value for T_i would be obtained for a wide range of values of P_j. In fact, when the sensitivity coefficients

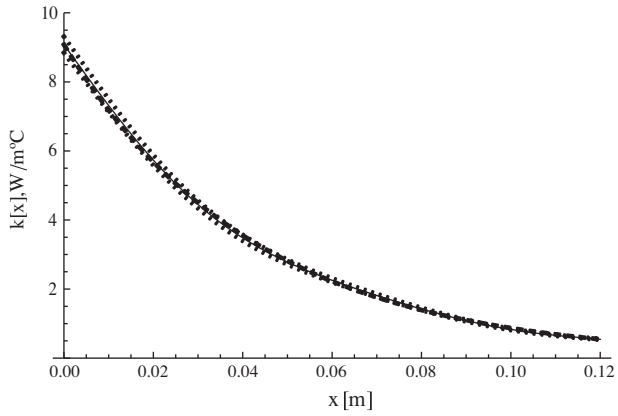

(a) Thermal conductivity

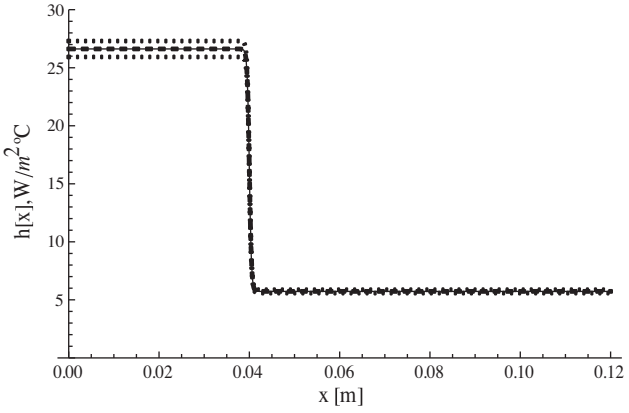

(c) Effective heat transfer coefficient

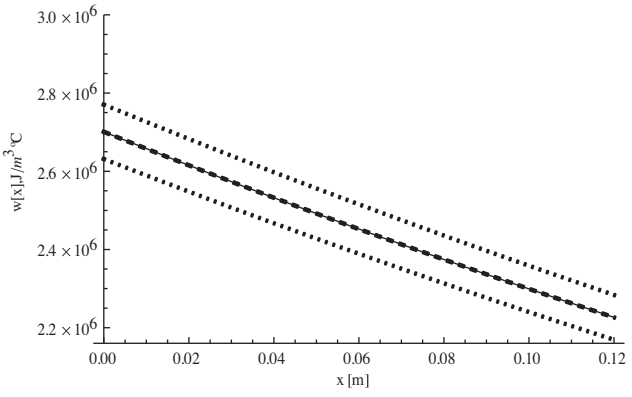

(b) Volumetric heat capacity

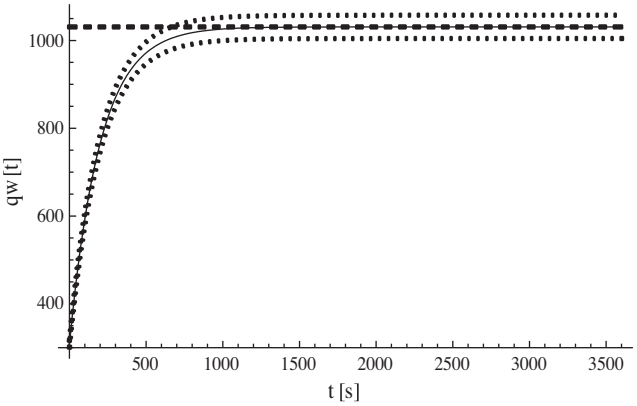

(d) Time lag function in applied heat flux

Fig. 6. Estimation results – test case 1.

are small, $|\mathbf{J}^T\mathbf{J}| \approx 0$ and the inverse problem is ill-conditioned. It can also be shown that $|\mathbf{J}^T\mathbf{J}|$ is null if any column of $\mathbf{J}$ can be expressed as a linear combination of other columns [32].

Table 3a presents different possibilities for the number of sensors, depending on the resolution of the infrared camera utilized, and the total number of experimental points available for a total of 300 measurements in time. As we can see, the total number of experimental points can be quite large with such kind of non-intrusive measurement instrument, which has encouraged the present approach of data compression in the spatial domain. With such an approach, the measured data points are not simply discarded, but compressed with the integral transformation of the measurements in the spatial domain, thus significantly reducing the amount of information to be actually handled by the inverse problem algorithm. Table 3b provides three cases involving different choices of parameters to be estimated, yielding a total number of $N_P = 11$, 15 or 19. The differences among such cases are basically associated with the increasing number of terms in the thermophysical properties eigenfunction expansions, $k(x)$ e $w(x)$. For the dissipation function $d(x)$, only one term was used in the eigenfunction expansion, since the adopted filter for this coefficient was already quite informative.

The integral transformation of the experimental data was performed in accordance with Eq. (18a), after interpolating the spatial measured data with cubic splines. In the inverse analysis that follows, 241 spatial measurements were employed in the integral transformation of the experimental data (see Table 3a). A considerable reduction on the experimental data set is then achieved with the integral transformation, as illustrated in Table 4. This table shows the total number of experimental points, for a fixed number of sensors (241), available for the estimation procedure performed directly in the temperature field. It also shows the number of data points available for the transformed measurement field, by varying the number of eigenmodes used in the transformations ($NT = 10$, 20, and 40). It can be noticed that a reduction of more than 10 times is achieved when the plain temperature data is replaced by the transformed temperature field with the truncation order of $NT = 20$.

Fig. 4 presents the determinant of the information matrix by using the integral transformed data in the inverse analysis. We can notice that the increase in the expansion truncation orders leads to an increase in the values of the determinant, as a result of the larger number of experimental points in the transformed domain. The three curves shown in Fig. 4, correspond from top to bottom to $NT = 40$, 20, and 10. On the other hand, by doubling the number of eigenmodes available for the transformed data a relatively small increase is observed in the determinant values for a fixed number of measurements in time. Therefore, for the results presented hereafter, we preferred to perform the inverse problem solution by keeping $NT = 10$ eigenmodes.

Fig. 5a shows the simulated experimental temperature data with the 0.5 °C uncertainty level, for selected times along the plate. For the sake of comparison, Fig. 5b illustrates the time evolution of the first 10 transformed temperature fields, again for the 0.5 °C uncertainty case. This figure shows the more significant role of the first five transformed temperatures.

The four test cases examined in this work are summarized in Table 5. Test cases 1 and 2 were chosen for validation purposes,

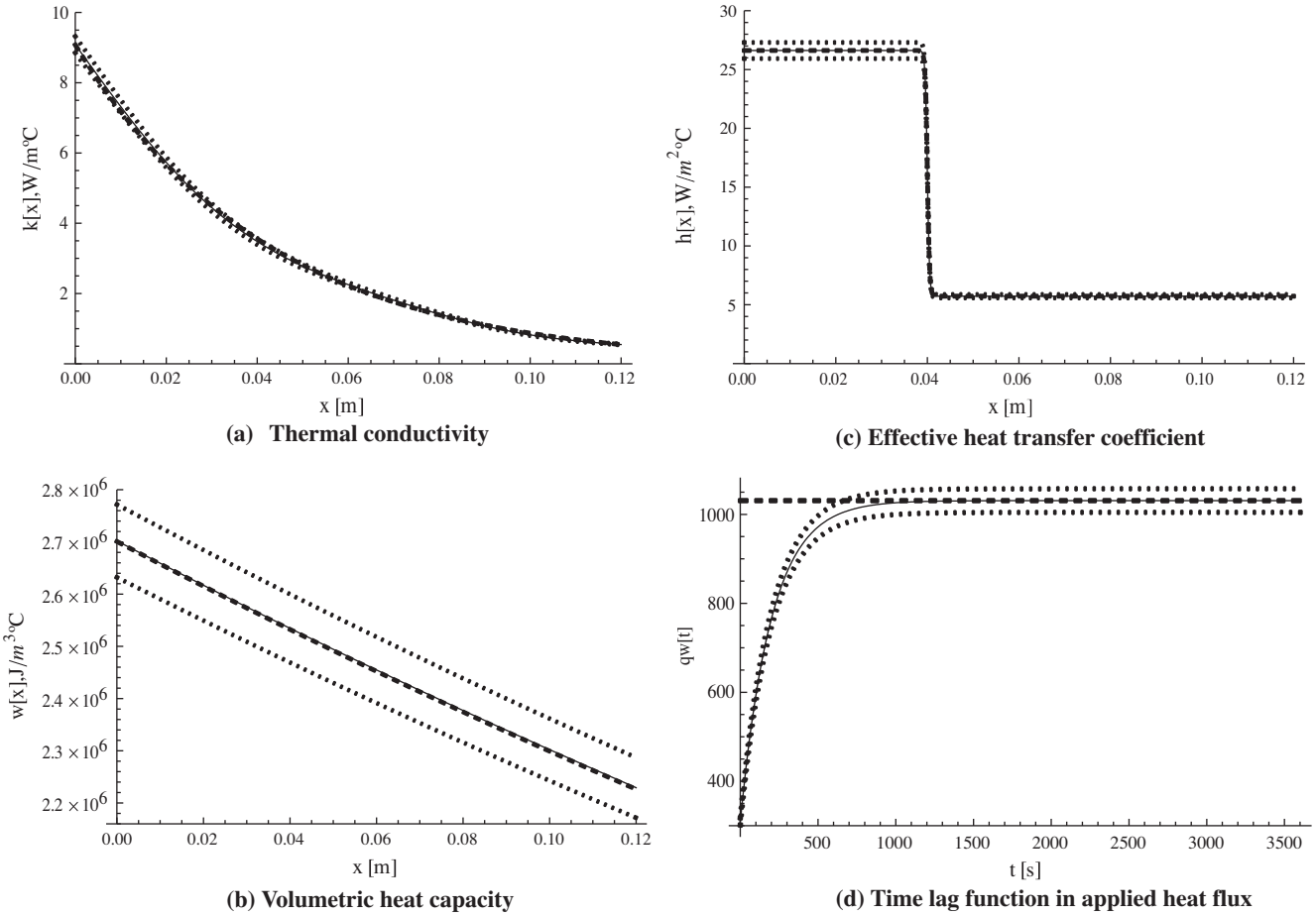

Fig. 7. Estimation results – test case 2.

since the experimental data were generated with the same number of terms in the expansions that were employed in the estimations, $NT = 10$, $N_k = 3$, $N_w = 3$, and $N_d = 1$, respectively for $T(x, t)$, $k(x)$, $w(x)$ and $d(x)$. The difference between test cases 1 and 2 is the different level of experimental error that was examined, an uncertainty of 0.0001 °C and of 0.5 °C, respectively. For the more challenging test cases 3 and 4, the experimental data were generated with $NT = 50$, $N_k = 10$, $N_w = 10$, and $N_d = 10$ and an uncertainty of 0.1 °C and 0.5 °C, respectively, while the estimation was performed with the same reduced number of terms as in test cases 1 and 2 to avoid the so called inverse crime. In these four test cases a uniform non-informative prior (denoted by U) was utilized for the transformed coefficients of the two thermophysical properties and of the linear dissipation coefficient, besides the two heat flux parameters a and b. Gaussian prior distributions (denoted by N) were adopted for the values of thermophysical properties and of the dissipation coefficient at the boundaries, centered at the expected values for each parameter, with a standard deviation of 5% of the respective exact value for k_{x0}, k_{xL}, w_{x0} and w_{xL} and of 20% for d_{x0} and d_{xL}. The uniform priors are defined with the minimum and maximum allowable limits in the search procedure, as detailed in Table 6. Table 6 also presents the expected exact values used to generate the simulated measurements, the upper and lower allowable bounds and the initial states used in the Markov chain for each parameter. As initial state of the Markov chain for these coefficients, we have chosen a random value of the coefficient in the range defined by 90% and 110% of the exact value. The maximum and minimum values for the coefficients to be estimated are obtained from the corresponding maximum and minimum values of the original coefficients, for instance, $k_{\max}$ and $k_{\min}$. The parameterized form of the thermal conductivity, as an example, is given by:

$$k(x) = \left(\frac{k_{x=L} - k_{x=0}}{L}\right)x + k_{x=0} + \sum_{k=1}^{N_k} \bar{k}_k \tilde{\Gamma}_k(x) \tag{24a}$$

or,

$$\sum_{k=1}^{N_k} \bar{k}_k \tilde{\Gamma}_k(x) = k(x) - \left(\frac{k_{x=L} - k_{x=0}}{L}\right)x - k_{x=0} \tag{24b}$$

By operating (24b) with $\int_0^L \tilde{\Gamma}_i(x)dx$ on both sides, we obtain:

$$\bar{k}_i = \int_0^L \tilde{\Gamma}_i(x)k(x)dx - \left(\frac{k_{x=L} - k_{x=0}}{L}\right)\bar{g}_i - k_{x=0}\bar{f}_i \tag{25a}$$

where

$$\bar{g}_i = \int_0^L x\tilde{\Gamma}_i(x)dx, \quad \bar{f}_i = \int_0^L \tilde{\Gamma}_i(x)dx \tag{25b, c}$$

Thus, for a bound maximum or minimum values of $k(x)$, $k_b = k_{\min}$ or $k_b = k_{\max}$, respectively, we have:

$$\bar{k}_{i,b} = (k_b - k_{x=0})\bar{f}_i - \left(\frac{k_{x=L} - k_{x=0}}{L}\right)\bar{g}_i \tag{26}$$

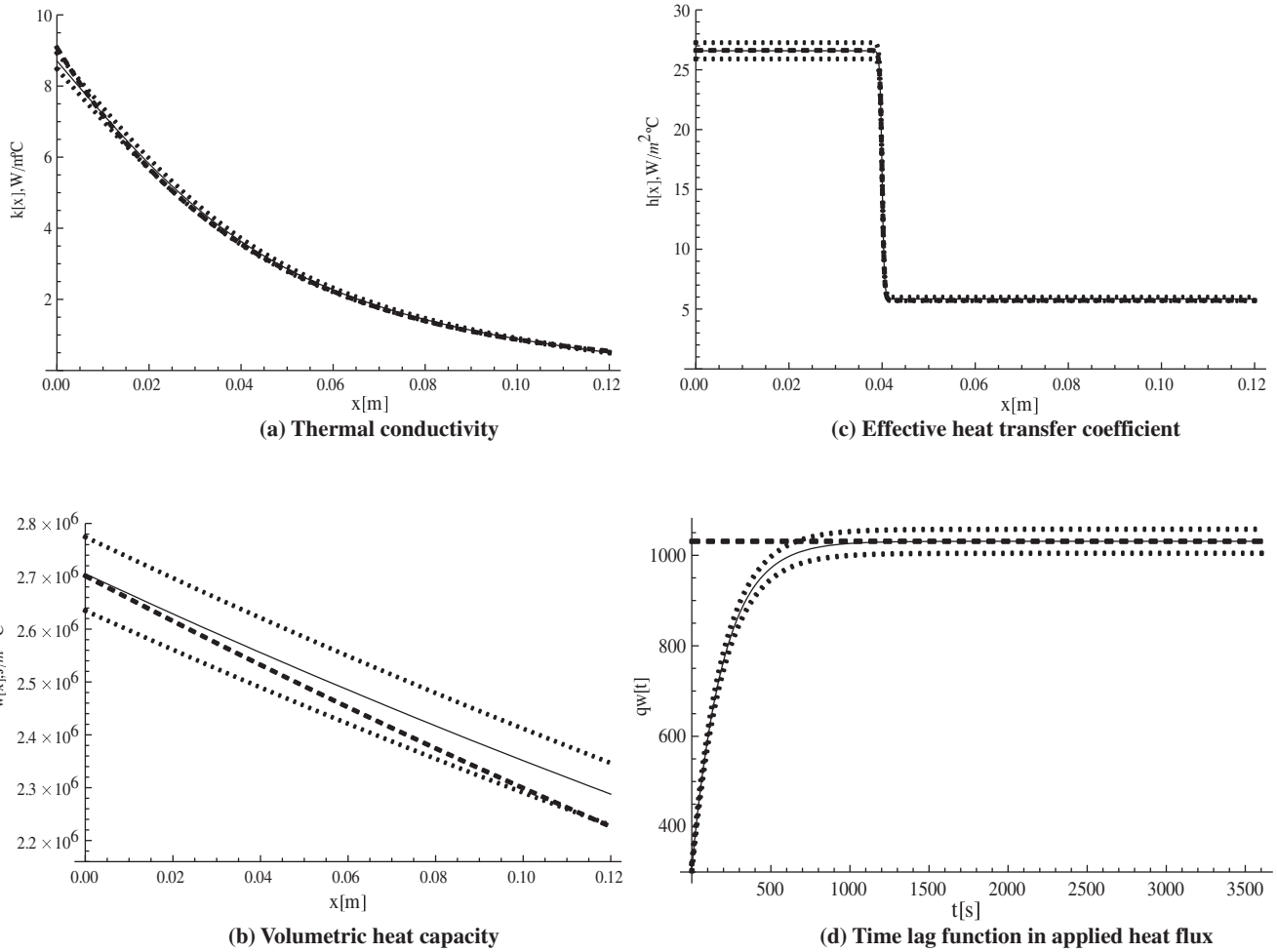

(a) Thermal conductivity

(c) Effective heat transfer coefficient

(b) Volumetric heat capacity

(d) Time lag function in applied heat flux

Fig. 8. Estimation results – test case 3.

Since the values of the original coefficients at the boundaries are not known *a priori*, to either maximize or minimize the values of the transformed coefficients in Eq. (26), we need to take into consideration the signs of the coefficients $\bar{g}_i$ and $\bar{f}_i$. Thus, from the analysis of the expression above, and the specific forms of the transformed quantities, $\bar{g}_i$ and $\bar{f}_i$ for odd or even indices, one may get conservative upper and lower limits for the expansion coefficients, for instance, $\bar{k}_{i,\max}$ and $\bar{k}_{i,\min}$, in the form:

for $i = \text{odd} \rightarrow (k_{x=0} = k_{x=L} = k_{\min}; k_b = k_{\max})$:

$$\bar{k}_{i,\max} = \frac{2\sqrt{2}(k_{\max} - k_{\min})}{i\pi\sqrt{1/L}} \tag{27a}$$

$$\bar{k}_{i,\min} = \frac{2\sqrt{2}(k_{\max} - k_{\min})}{i\pi\sqrt{1/L}} \tag{27b}$$

for i = even $\rightarrow (k_{x=0} = k_{\min};\ k_{x=L} = k_{\max})$

$$\bar{k}_{i,\max} = \frac{2(k_{\max} - k_{\min})}{i\pi\sqrt{1/L}} \tag{28a}$$

for i = even $\rightarrow (k_{x=L} = k_{\min};\ k_{x=0} = k_{\max})$

$$\bar{k}_{i,\min} = \frac{-\sqrt{2}(k_{\max} - k_{\min})}{i\pi\sqrt{1/L}} \tag{28b}$$

Alternatively, a priori information on the coefficients could have been used to narrow the minimum to maximum intervals, but at the present stage of tools demonstration, we have preferred to employ a wider range.

Figs. 6–9 present the results obtained in the estimations procedure for the four test cases, where the dashed lines represent the expected exact function, the solid lines represent the estimated functions, and the dotted lines represent the lower and upper limits related to the 99% confidence levels after propagating the uncertainties involved in the reconstruction of the functions. Only for the figures related to the time lag of the applied heat flux, the dashed lines represent just the steady-state expected value of the prescribed heat flux, q_{inf}.

From the analysis of Figs. 6a–d and 7a–d, related to the two validations cases 1 and 2, one may observe that the proposed approach was able to recover by estimation the expected exact functions, thus validating the proposed procedure based on the integral transformed temperature data. Even for the higher error level of 0.5 C (case 2), the estimations remain practically coincident to the graph scale with the expected exact coefficients behavior. Therefore, the data compression through the integral transformation of the measured data, which was introduced in this work, does not affect the spatial information conveyed by the local temperature measurements, and is still capable of resulting in very accurate estimations for the functions. The analysis of the results for the more challenging test cases 3 and 4, presented in Figs. 8a–d and 9a–d, with uncertainty of the temperature measurements of 0.1 C and 0.5 C, respectively, reveals that better estimates are achieved with the use of the 0.1C error level (test case 3). Nevertheless, the results obtained for test case 4 (Fig. 9a–d), with a much higher error level of 0.5 C, demonstrate that the present approach, even in such case, can still provide reasonable estimates. Only at the cooler edge of the plate, where the temperature distribution

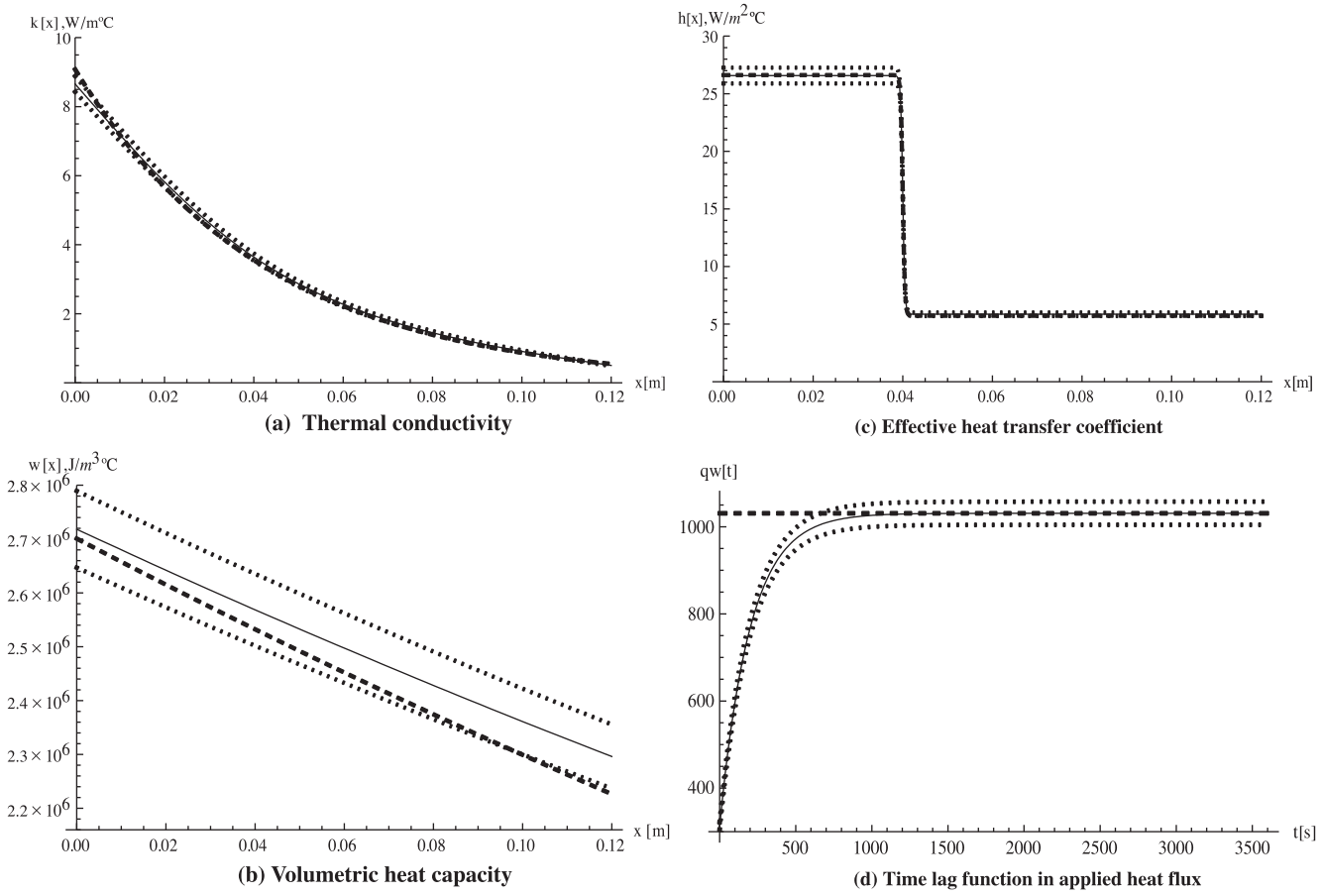

Fig. 9. Estimation results – test case 4. (a) Thermal conductivity; (b) volumetric heat capacity and (c) effective heat transfer coefficient; (d) time lag function in applied heat flux.

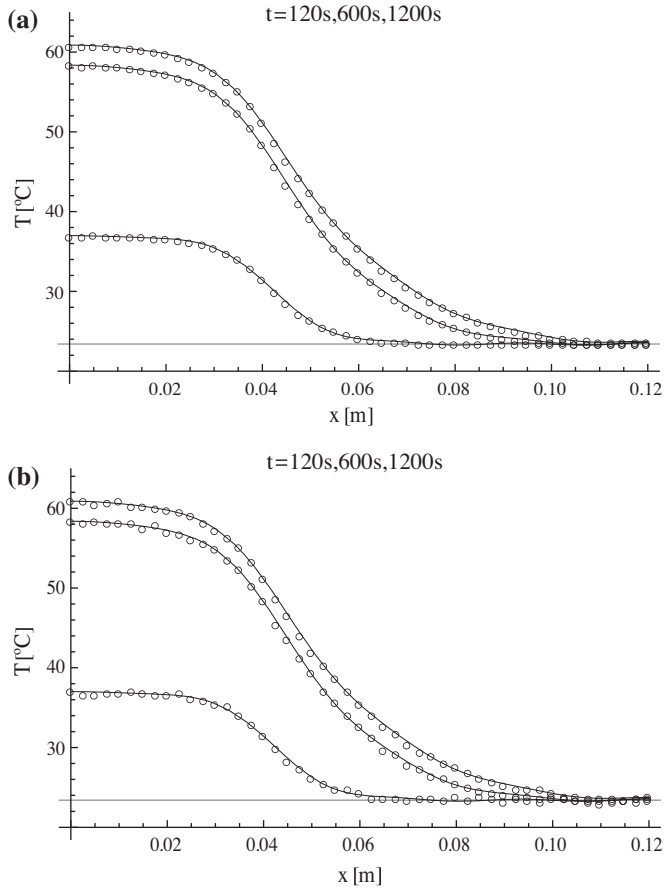

Fig. 10. Comparison between experimental and estimated temperatures at different times for test case 3 (a) and test case 4 (b).

is practically unchanged along the transient (see Fig. 10), the estimation of the thermal capacity boundary value, present in the filter solution for this function, is more challenged in both cases 3 and 4. The encouraging performance of the proposed inverse analysis is also clear from the excellent agreement achieved between the experimental and estimated temperatures, for both test cases 3 and 4, as demonstrated by Fig. 10a, for case 3, and Fig. 10b for case 4, for the times t = 120 s, 600 s and 1200 s. In these curves, not to overpopulate the graphs with the experimental data, the dots represent the experimental temperature measurements at every five time steps.

6. Conclusions

The present work addresses the inverse analysis for the simultaneous identification of space variable thermophysical properties in heterogeneous materials, together with the estimation of boundary condition coefficients in a heat conduction problem. From the experience achieved in previous contributions, the direct problem solution was analytically obtained through integral transforms, with the related eigenvalue problem solved by the Generalized Integral Transform Technique (GITT). The unknown variables to be estimated were also expanded in terms of eigenfunctions, yielding a straightforward parameterization of the functions to be identified, besides a fully analytical implementation of the coefficients matrix in the direct problem solution. Bayesian inference is employed in the inverse problem solution, implemented via the Monte Carlo Markov Chain method and the Metropolis-Hastings sampling procedure. The proposed approach also introduces the use of experimental information in the transformed domain. The discrete temperature measurements along the space coordinate are integral transformed into a small set of modes which represent the experimental transformed temperatures. A remarkable data compression is achieved through this transformation procedure, thus significantly accelerating the inverse problem algorithm, without loss of information for the reconstruction of the local thermophysical properties spatial behavior. The approach here implemented can in principle be directly extended to multidimensional cases, thus taking further advantage of the large amount of spatially distributed measurements normally made available through thermographic cameras.

Acknowledgements

The authors would like to acknowledge the financial support provided by CNPq, CAPES and FAPERJ, Brazilian agencies for the fostering of sciences. This work was performed along several months of pain and suffering, for the premature loss of our beloved ones, Bianca Cotta and Carlos Eduardo, the day after their "fairy-tale" marriage. Our strength to overcome this period came from the support of a real army of relatives and friends, all over the world, to whom we dedicate this effort.

References

[1] S.H. Lin, Transient Conduction in Heterogeneous Media, Int. Commun. Heat Mass Transfer 10 (1992) 165–174.
[2] E. Divo, A. Kassab, Generalized boundary integral equation for transient heat conduction in heterogeneous media, J. Thermophys. Heat Transfer 12 (1998) 364.
[3] O. Fudym, B. Ladevie, J.C. Batsale, A seminumerical approach for heat diffusion in heterogeneous media: one extension of the analytical quadrupole method, Numer. Heat Transfer, Part B: Fundam. 42 (2002) 325–348.
[4] B. Chen, L. Tong, Y. Gu, H. Zhang, O. Ochoa, Transient heat transfer analysis of functionally graded materials using adaptive precise time integration and graded finite elements, Numer. Heat Transfer, Part B 45 (2) (2004) 181–200.
[5] D. Kumlutas, I.H. Tavman, A numerical and experimental study on thermal conductivity of particle filled polymer composites, J. Thermoplast. Compos. Mater. 19 (2006) 441–455.
[6] J. Fang, G.F. Zhao, J. Zhao, A. Parriaux, On the truly meshless solution of heat conduction problems in heterogeneous media, Numer. Heat Transfer, Part B 55 (1) (2009) 1–13.
[7] R.C. Progelhof, J.L. Throne, R.R. Ruetsch, Methods for predicting the thermal conductivity of composite systems: a review, Polym. Eng. Sci. 16 (9) (1976) 615–625.
[8] I.H. Tavman, Thermal and mechanical properties of aluminum powder-filled high-density polyethylene composites, J. Appl. Polym. Sci. 62 (1996) 2161–2167.
[9] I.H. Tavman, H. Akinci, Transverse thermal conductivity of fiber reinforced polymer composites, Int. Commun. Heat Mass Transfer 27 (2000) 253–261.
[10] D. Kumlutas, I.H. Tavman, M.T. Çoban, Thermal conductivity of particle filled polyethylene composite materials, Compos. Sci. Technol. 63 (1) (2003) 113–117.
[11] F. Danes, B. Garnier, T. Dupuis, Predicting, measuring and tailoring the transverse thermal conductivity of composites from polymer matrix and metal filler, Int. J. Thermophys. 24 (2003) 771–784.
[12] B. Weidenfeller, M. Hofer, F.R. Schilling, Thermal conductivity, thermal diffusivity, and specific heat capacity of particle filled polypropylene, Composites, Part A 35 (2004) 423–429.
[13] H. Serkan Tekce, D. Kumlutas, I.H. Tavman, Effect of particle shape on thermal conductivity of copper reinforced polymer composites, J. Reinforced Plast. Compos. 26 (2007) 113–121.
[14] M.D. Mikhailov, M.N. Ozisik, Unified Analysis and Solutions of Heat and Mass Diffusion, John Wiley, NY, 1984.
[15] R.M. Cotta, M.N. Ozisik, Laminar forced convection in ducts with periodic variation of inlet temperature, Int. J. Heat Mass Transfer 29 (1986) 1495–1501.
[16] R.M. Cotta, Hybrid numerical–analytical approach to nonlinear diffusion problems, Numer. Heat Transfer, Part B 127 (1990) 217–226.
[17] R.M. Cotta, Integral Transforms in Computational Heat and Fluid Flow, CRC Press, USA, 1993.
[18] R.M. Cotta, M.D. Mikhailov, Heat Conduction: Lumped Analysis, Integral Transforms, Symbolic Computation, Wiley-Interscience, NY, 1997.
[19] R.M. Cotta, The Integral Transform Method in Thermal and Fluids Sciences and Engineering, Begell House, New York, 1998.
[20] R.M. Cotta, M.D. Mikhailov, Hybrid Methods and Symbolic Computations, in: W.J. Minkowycz, E.M. Sparrow, J.Y. Murthy (Eds.), Handbook of Numerical Heat Transfer, second ed., Wiley, New York, 2006, pp. 493–522.

[21] L.A. Sphaier, R.M. Cotta, C.P. Naveira-Cotta, J.N.N. Quaresma, The UNIT (unified integral transforms) symbolic- numerical computational platform for benchmarks in convection–diffusion problems, in: Proceedings of the 30th CILAMCE, 30th Iberian–Latin–American Congress on Computational Methods in Engineering, Búzios, RJ, Brasil, November 2009.
[22] G.P. Flach, M.N. Ozisik, Inverse heat conduction problem of simultaneously estimating spatially varying thermal conduction and heat capacity per unit volume, Numer. Heat Transfer, Part A: Appl. 16 (1989) 249–266.
[23] C.H. Huang, M.N. Ozisik, A direct integration approach for simultaneously estimating spatially varying thermal conductivity and heat capacity, Int. J. Heat Fluid Flow 11 (3) (1990) 262–268.
[24] D. Lesnic, L. Elliot, D.B. Ingham, B. Clennell, R.J. Knioe, The identification of the piecewise homogeneous thermal conductivity of conductors subjected to a heat flow test, Int. J. Heat Mass Transfer 42 (1999) 143–152.
[25] E. Divo, A. Kassab, F. Rodriguez, Characterization of space dependent thermal conductivity with a BEM-based genetic algorithm, Numer. Heat Transfer, Part A 37 (2000) 845–875.
[26] C.H. Huang, S.C. Chin, A two-dimensional inverse problem in imaging the thermal conductivity of a non-homogeneous medium, Int. J. Heat Mass Transfer 43 (2000) 4061–4071.
[27] F.A. Rodrigues, H.R.B. Orlande, G.S. Dulikravich, Simultaneous estimation of spatially dependent diffusion coefficient and source term in a nonlinear 1D diffusion problem, Math. Comput. Simul. 66 (2004) 409–424.
[28] J.M.J. Huttunen, T. Huttunen, M. Malinen, J. Kaipio, Determination of heterogeneous thermal parameters using ultrasound induced heating and MR thermal mapping, Phys. Med. Biol. 51 (2006) 1011–1032.
[29] C.H. Huang, C.Y. Huang, An inverse problem in estimating simultaneously the effective thermal conductivity and volumetric heat capacity of biological tissue, Appl. Math. Model. 31 (2007) 1785–1797.
[30] J.V. Beck, K. Arnold, Parameter Estimation in Engineering and Science, Wiley-Interscience, New York, 1977.
[31] O.M. Alifanov, Inverse Heat Transfer Problems, Springer-Verlag, New York, 1994.
[32] M.N. Ozisikm, H.R.B. Orlande, Inverse Heat Transfer: Fundamentals and Applications, Taylor and Francis, New York, 2000.
[33] J. Kaipio, E. Somersalo, Statistical and Computational Inverse Problems, Springer-Verlag, 2004.
[34] N. Zabaras, Inverse problems in heat transfer, in: W.J. Minkowycz, E.M. Sparrow, J.Y. Murthy (Eds.), Handbook of Numerical Heat Transfer, second ed., Wiley, New York, 2006, pp. 525–557.
[35] D. Gamerman, H.F. Lopes, Markov chain Monte Carlo: stochastic simulation for Bayesian inference, second ed., Chapman & Hall/CRC, 2006.
[36] H.S. Migon, D. Gamerman, Statistical Inference: An Integrated Approach, Arnold/Oxford, London/New York, 1999.
[37] H.R.B. Orlande, M.J. Colaço, G.S. Dulikravich, Approximation of the likelihood function in the Bayesian technique for the solution of inverse problems, Inverse Probl. Sci. Eng. 16 (2008) 677–692.
[38] O. Fudym, H.R.B. Orlande, M. Bamford, J.C. Batsale, Bayesian approach for thermal diffusivity mapping from infrared images processing with spatially random heat pulse heating, J. Phys. Conf. Ser. (Online) 135 (2008) 12–42.
[39] N. Metropolis, A.W. Rosenbluth, M.N. Rosenbluth, A.H. Teller, E. Teller, Equations of state calculations by fast computing machines, J. Chem. Phys. 21 (1953) 1087–1092.
[40] W.K. Hastings, Monte Carlo sampling methods using Markov chains and their applications, Biometrika 57 (1970) 97–109.
[41] S. Wolfram, The Mathematica Book, version 5.2, Cambridge-Wolfram Media, 2005.
[42] C.P. Naveira-Cotta, R.M. Cotta, H.R.B. Orlande, O. Fudym, Eigenfunction expansions for transient diffusion in heterogeneous media, Int. J. Heat Mass Transfer 52 (2009) 5029–5039.
[43] M.D. Mikhailov, R.M. Cotta, Integral transform method for eigenvalue problems, Commun. Numer. Methods Eng. 10 (1994) 827–835.
[44] L.A. Sphaier, R.M. Cotta, Integral transform analysis of multidimensional eigenvalue problems within irregular domains, Numer. Heat Transfer, Part B: Fundam. 38 (2000) 157–175.
[45] C.P. Naveira-Cotta, H.R.B. Orlande, R.M. Cotta, Integral transforms and Bayesian inference in the identification of variable thermal conductivity in two-phase dispersed systems, Numer. Heat Transfer, Part B: Fundam. 57 (3) (2010) 1–30.